RSC Advances

PAPER

View Article Online
View Journal | View Issue

Cite this: *RSC Adv.*, 2017, **7**, 25101

A robust duplex Cu/PDMS-coated mesh with superhydrophobic surface for applications in cleaning of spilled oil†

Jingfang Zhu, [a] Liyun Wu,[a] Jingjing Li,[a] Bin Liu*[a] and Zhixiang Zeng*[b]

Received 5th January 2017
Accepted 18th April 2017

DOI: 10.1039/c7ra00150a

rsc.li/rsc-advances

In this study, we created a robust and stable nanostructure coated on the surface of a stainless steel mesh *via* the electrodeposition of copper thin films and chemical modification with polydimethylsiloxane (PDMS) to enhance the mechanical durability of the stainless steel mesh surface with superhydrophobic performance. The obtained stainless steel mesh was tested by immersion in solutions of different pH values and abrasion cycling tests with sandpaper. The results showed that the coated stainless steel mesh retained excellent superhydrophobic and superoleophilic properties. Using the superhydrophobic and superoleophilic stainless steel mesh, we achieved the recycling of oil automatically and continuously *via* a vacuum pump.

1. Introduction

As evolved by nature, the surface of lotus leaves has an intriguing self-cleaning character.[1,2] Therefore, the development of multifunctional and applied materials with superhydrophobic character has evoked great interest because of their potential applications in anti-icing,[3,4] heat transfer,[5,6] drag reduction,[7,8] antifogging[2,9] and anticorrosion technologies,[10,11] and so on. However, oil/water separation is a major potential application, which could be used for the cleanup of oil spills. Both low surface energy and rough surface structures are the main influencing factors of superhydrophobicity.[12,13] Various filtration materials with superhydrophobicity and superoleophilicity, such as textiles,[14] meshes,[15] cellulose sponges,[16] and membranes,[17] have been fabricated to selectively filter water or oil from oil/water mixtures. Among artificial superhydrophobic materials,[18–22] as-prepared mesh surfaces with superhydrophobic character have been some of the most promising examples owing to their strong water repellence, which endowed hierarchical surfaces with robust superhydrophobicity and uses in practical applications.

Recently, many studies have reported the cleaning up of oil spills.[23] Previous studies might have been more reasonable if they had considered issues such as the mechanical strength of superhydrophobic surfaces, complex multi-step processing, high-temperature treatment, recontamination, and oil recovery *via* tedious mechanical squeezing.[24,25] Therefore, the appropriate treatment of oil spill accidents has still remained an inevitable technological challenge in practical applications.

As-prepared mesh surfaces with superhydrophobic and superoleophilic character were widely used in oil/water separation because of their good mechanical properties.[26–28] For example, Jiang *et al.* fabricated a stable superhydrophobic and superoleophilic ZnO-coated stainless steel mesh film with special hierarchical micro/nanostructures.[29] Kota *et al.* fabricated microbeads on textured surfaces *via* a single-step technique to develop superoleophobic surfaces.[30] The strength of superhydrophobic surfaces played an important role in practical applications. In comparison with superwetting sponges, these novel devices could collect and recycle oil without an extrusion process. Therefore, rapid, highly effective, antiabrasive, mechanically durable, and green materials and techniques were needed for the treatment of oil spills in harsh marine environments. To the best of our knowledge, very few reports have been published on the electrodeposition of copper thin films and chemical modification with PDMS to improve the robust mechanical properties of superhydrophobic mesh surfaces in the area of oil/water separation applications. Previous studies demonstrated that the preparation process *via* one-step immersion is convenient and simple.[15] In this article, a superhydrophobic and superoleophilic mesh with hierarchical micro/nanostructures was fabricated *via* a green, rapid, and highly effective electrodeposition process and chemical modification with PDMS. The porous coated mesh retained excellent superhydrophobicity after immersion in solutions of different pH values and abrasion cycling tests. Therefore, this

[a]*School of Materials Science and Engineering, North University of China, Taiyuan 030051, People's Republic of China. E-mail: liubin3y@nuc.edu.cn; Tel: +86-0351-3557423*

[b]*Key Laboratory of Marine Materials and Related Technologies, Zhejiang Key Laboratory of Marine Materials and Protective Technologies, Ningbo Institute of Materials Technology and Engineering, Chinese Academy of Sciences, Ningbo 315201, People's Republic of China. E-mail: zengzhx@nimte.ac.cn; Tel: +86-0574-86685809*

† Electronic supplementary information (ESI) available. See DOI: 10.1039/c7ra00150a

study offers a new strategy for treating oil spills, which could be potentially used in the future as an advanced technology in the petrochemical industry.

2. Experimental

2.1. Materials

The reagents were purchased from Aladdin Reagent. The samples of (304) stainless steel mesh used as substrates were purchased from Shanghai Xinyan Metal Mesh Factory, China. The polydimethylsiloxane (PDMS) and curing agent were purchased from Dow Corning.

2.2. Sample preparation

Preparation of mesh/Cu-coated. Pretreated samples of (304) stainless steel mesh were immersed in solutions of hydrochloric acid, acetone, and ethanol, respectively. The preparation of mesh/Cu-coated was carried out at a current density of 0.5 mA cm^{-2} on a stainless steel mesh substrate in an electrolytic bath containing 0.8 M $CuSO_4 \cdot 5H_2O$ and 0.5 M H_2SO_4. All the electrolytes were prepared using analytical-grade reagents and deionized (DI) water. The electrodeposition was conducted at room temperature in a two-electrode electrochemical cell with a Cu plate as the anode and a stainless steel mesh as the cathode. During deposition, the electrolyte was stirred with a magnetic stirrer.

Preparation of mesh/Cu/PDMS-coated. After electrodeposition, mesh/Cu-coated was immersed in a mixture of PDMS and a curing agent in a 10 : 1 ratio and ethyl acetate. The detailed process was as follows: the thickness of the PDMS film was achieved by repeated immersion and drying. Finally, mesh/Cu/PDMS-coated with superhydrophobic and superoleophilic character was treated at 80 °C for 3 h. The detailed preparation process of the sample is graphically displayed in Scheme 1.

2.3. Characterization

The surface topographies of samples were scanned using scanning electron microscopy (SEM) (FEI Quanta 250 FEG, US) at an accelerating voltage of 10 kV, and the mesh/PDMS and mesh/Cu/PDMS-coated surfaces were sputtered with a thin layer of gold to avoid the accumulation of charge. X-ray photoelectron spectroscopy (XPS) was carried out with an AXIS Ultra DLD spectrometer (Kratos, Japan). The chemical compositions of the mesh surfaces were examined by EDS. The apparent contact angles (CAs) of samples were measured using a video contact angle measurement system (OCA20, Germany) with a water droplet (5.0 μL) and an oil droplet (5.0 μL), respectively. The CAs of the samples were measured for every mesh surface at least four times, and the average value was recorded.

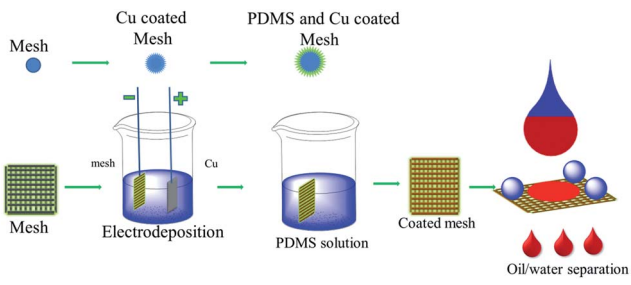

Scheme 1 Fabrication process of superhydrophobic and superoleophilic stainless steel mesh for application in oil/water separation.

3. Results and discussion

To fabricate a superhydrophobic surface on the porous mesh, we constructed hierarchical micro/nanostructures on the surface of the porous stainless steel mesh *via* a facile one-step electrodeposition method. The different surface topographies of the samples were investigated in experiments on mesh/Cu, mesh/PDMS, and mesh/Cu/PDMS films, respectively, as shown in Fig. 1. SEM images at different magnifications of the mesh/Cu thin film after electrodeposition treatment in the solution of $CuSO_4$ and H_2SO_4 are shown in Fig. 1(a)–(c). It can be seen in Fig. 1(a) that the mesh surface film comprised a layer of rough and uniform nanoparticles after electrodeposition. The higher-magnification images in Fig. 1(b) and (c) show that mesh/Cu-coated formed a typical hierarchical micro/nanostructure with pyramid-like shapes. The particles in Fig. 1(b) have a thickness of about ~22 μm on average. The lengths of Cu-coated particles were about ~12 μm, as shown in Fig. S1,† and there were many hierarchical grooves on the surface of mesh/Cu-coated. Moreover, the one-step electrodeposition method was green, facile, and robust and constructed Cu-coated hierarchical micro/nanostructures on various substrates. (These hierarchical rough micro/nanostructures on the mesh surface were essential for superhydrophobicity.) Fluorine-containing compounds are toxic and costly. Therefore, we provided a layer of cross-linked PDMS thin films for the mesh surface to decrease the surface energy, which was a simple, green process, as shown in the SEM images in Fig. 1(d)–(f), and the cross-sectional morphologies of mesh/Cu/PDMS-coated are shown in Fig. S1.† The original mesh surface was very smooth with some thin PDMS films, as shown in Fig. 1(d). The Cu-coated mesh was covered by some thin PDMS films, as shown in Fig. 1(e) and (f). The wire diameter and pitch of the mesh were about 48 μm and 79 μm, respectively, as shown in Fig. S5.†

EDS analysis was conducted to study the chemical composition of pristine mesh and the coated meshes, namely, mesh/PDMS, mesh/Cu and mesh/Cu/PDMS. In comparison with pristine mesh (Fig. 2(a)), the EDS results showed that the mesh was covered with a Cu coating layer, as shown by the very strong Cu peak in Fig. 2(c), after electrodeposition treatment in the solution of $CuSO_4$ and H_2SO_4. The results showed that Cu-coated hierarchical micro/nanostructures were successfully electrodeposited on the mesh substrate. The superhydrophobic surface of lotus leaves has hierarchical micro/nanostructures and an extremely low surface energy simultaneously. In previous studies, to decrease the surface energy, the rough surface that was obtained was usually chemically modified with fluoride compounds to acquire superhydrophobicity. However, the fluoride compounds were toxic and caused secondary pollution. Therefore, we constructed a layer of cross-linked

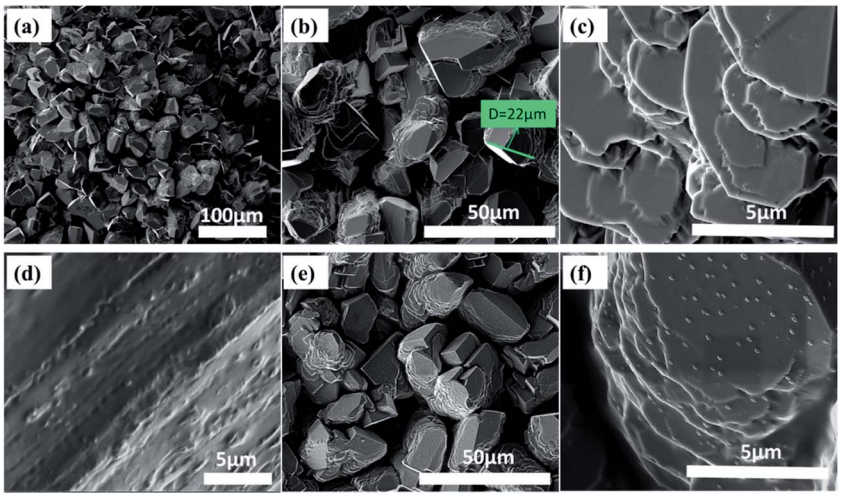

Fig. 1 SEM images at different magnifications of mesh/Cu-coated (a–c), mesh/PDMS-coated (d) and mesh/Cu/PDMS-coated (e and f), respectively.

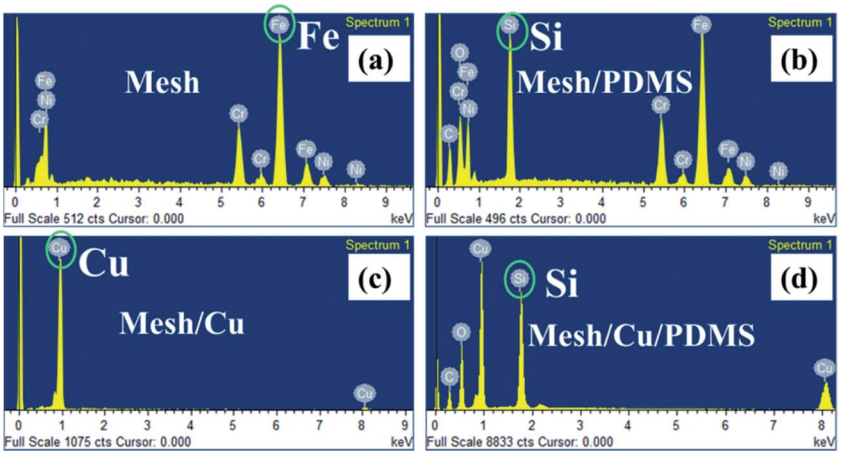

Fig. 2 Chemical composition of stainless steel meshes shown by EDS spectra of pristine mesh (a), mesh/PDMS-coated (b), mesh/Cu-coated (c) and mesh/Cu/PDMS-coated (d).

PDMS films on the Cu-coated surface to decrease the surface energy. As shown in the SEM images in Fig. 1(d)–(f), there was a layer of cross-linked PDMS films that was low-cost and green. The EDS results showed that mesh/PDMS (Fig. 2(b)) and mesh/Cu/PDMS (Fig. 2(d)) were covered with a layer of PDMS films, because there was a very strong Si peak, as shown in Fig. 2(b) and (d), after the coating treatment with PDMS. The content of every element in mesh/Cu/PDMS-coated is shown in Fig. 2(d). The contents of C, O, Si and Cu were 46.89%, 21.42%, 28.41%, and 3.29%, respectively, as shown in Fig. S4.† In contrast, there were no Si peaks for pristine mesh and mesh/Cu films, as shown in Fig. 2(a) and (c), which indicated that cross-linked PDMS had been successfully coated on the substrate. The chemical compositions of the Cu- and Cu/PDMS-coated meshes were analyzed using XPS. As shown in Fig. 3, the composition of the Cu-coated mesh included Cu, C, and O but not Si. The elements in the Cu/PDMS-coated mesh were Cu, C, O, and Si. The analyses indicated that the mesh surface was covered with a Cu/PDMS coating.[31]

To prove the superhydrophobicity of mesh/Cu/PDMS-coated, we observed the wettability by water of the surface of pristine mesh, mesh/Cu-coated, mesh/PDMS-coated, and mesh/Cu/

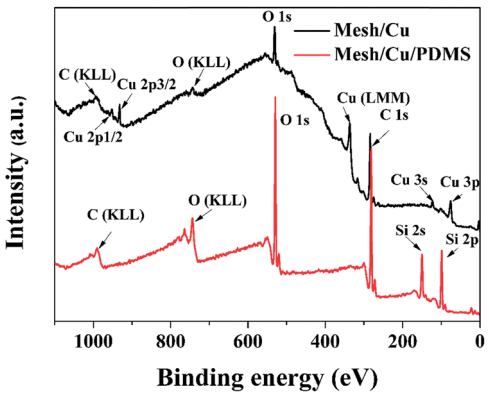

Fig. 3 XPS spectra of mesh/Cu and mesh/Cu/PDMS films.

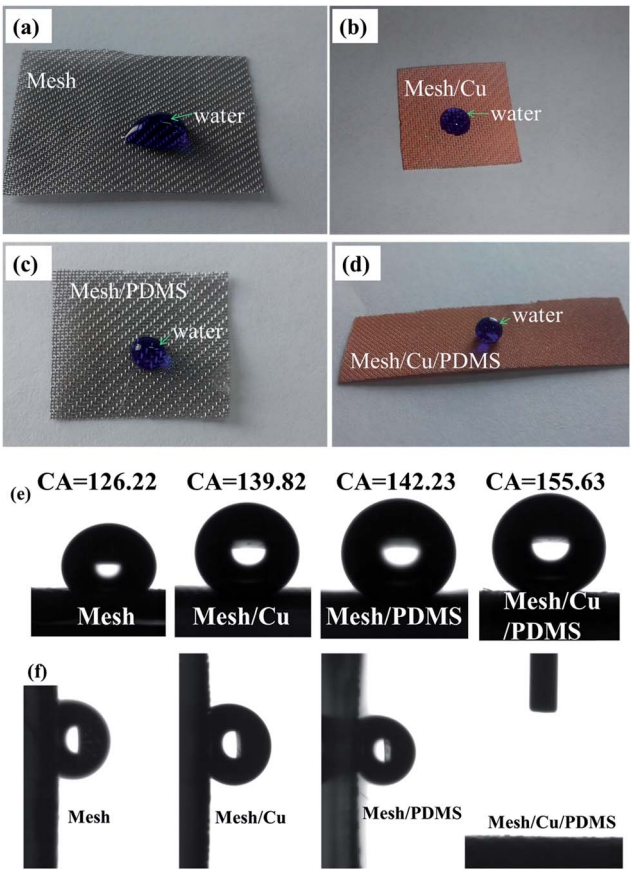

Fig. 4 Digital photos of various mesh surfaces showing the wetting state of water (a–d) and contact angles (e). (f) Water sliding angles of various coated mesh surfaces; mesh/Cu/PDMS was non-stick.

PDMS-coated, as shown in Fig. 4. In comparison with pristine mesh, as shown in Fig. 4(a) and (e), mesh/Cu coated with hierarchical structures had an apparent contact angle of water of 139.82°, as shown in Fig. 4(b) and (e), and was not superhydrophobic, because of the high surface energy of the mesh/Cu-coated surface. Pristine mesh that had been chemically modified with PDMS solution (mesh/PDMS-coated) had an apparent contact angle (CA) of a water droplet of 142.23°, as shown in Fig. 4(c) and (e). Mesh/Cu/PDMS-coated, which had a low surface energy and a hierarchical structure of Cu, had an apparent contact angle of a water droplet of 155.63°, as shown in Fig. 4(d) and (e), which was much higher than those of pristine mesh, mesh/PDMS-coated and mesh/Cu-coated. We measured the surface energy of mesh/Cu-coated and mesh/Cu/PDMS-coated by a dynamic contact angle measuring device. The surface energy of mesh/Cu-coated was 76.26 mN m^{-1}. After being coated with PDMS, the surface energy of mesh/Cu/PDMS-coated was 26.43 mN m^{-1}, as shown in Fig. 4(a)–(e), which indicated that the treatment effectively improved the hydrophobic property of pristine mesh. In Fig. 4(f), it can be seen that pristine mesh, mesh/Cu-coated and mesh/PDMS-coated substrates have strong adhesion properties. Water droplets on pristine mesh, mesh/Cu-coated and mesh/PDMS-coated surfaces could not roll down when the surfaces were tilted by 90°, which indicated that the droplets were in the Wenzel state. As on a low-adhesion surface, the droplet could very easily roll down from the mesh/Cu/PDMS-coated surface, which had a sliding angle of ~5.3°. This indicated that the surface roughness and low surface energy were essential for controlling the surface wettability.[32]

The superhydrophobic coated meshes have a low surface energy and high roughness, according to the Cassie–Baxter formula,[33–35] which can be written as:

$$\cos\theta = f(\cos\theta_E + 1) - 1 \quad (1)$$

where θ_E represents the (Young) contact angle of the flat surface, θ represents the apparent contact angle when droplets in the stable equilibrium state are present on the mesh surface, and f represents the areal fraction of droplets in contact with the mesh surface. The values of θ_E and θ were measured by a video contact angle measurement system and were found to be 126° and 156°, respectively. The calculated value of f was 20.9%, which indicated that the grooves on the mesh surface captured a large amount of air, and a micro/nanometer-scale composite structure was present on the surface of the samples. The contact of the droplets with the solid surface of the mesh changed into liquid–gas–solid contact, which greatly increased the apparent contact angle; furthermore, water droplets could bounce and roll off the surface. In addition, contact angle hysteresis plays a crucial role at solid–liquid interfaces. The concept of contact angle hysteresis θ_H ($\theta_H = \theta_A - \theta_R$) represents the difference between advancing (θ_A) and receding (θ_R) contact angles, as shown in Fig. 5(a). As a droplet expands, the maximum observed angle is the advancing contact angle θ_A, where the contact line remains until the droplet suddenly exceeds a critical volume. While the droplet shrinks, the contact line remains unchanged until the droplet shrinks below a critical volume. The minimum angle is the receding contact angle θ_R, as shown in Fig. 5(a), according to the sliding angle formula, which can be expressed as:

$$mg(\sin a)/w = \gamma_{AL}(\cos\theta_R - \cos\theta_A) \quad (2)$$

where m represents the mass of the droplet, g represents the acceleration due to gravity, a represents the angle of slope of the surface necessary to cause the droplet to slide, γ_{AL} represents the surface tension of the liquid droplet, w represents the width of the droplet, θ_A represents the advancing contact angle, and θ_R represents the receding contact angles. According to this formula, it is obvious that a droplet with a smaller difference between the advancing and receding contact angles (contact angle hysteresis) will give rise to a smaller sliding angle, as shown in Fig. 5(a) and (b). The relationship between the concentration of the PDMS solution and the wetting ability for mesh/Cu/PDMS-coated surfaces was researched, as shown in Fig. 5(c), and PDMS solutions with concentrations of 0.002, 0.006, 0.010, and 0.014 g mL^{-1} were used. The concept of contact angle hysteresis is equal to the difference between the advancing and receding contact angles. The contact angle hysteresis of a water droplet was within the range of 5.3–13.2°, as shown in Fig. 5(c). With an increase in

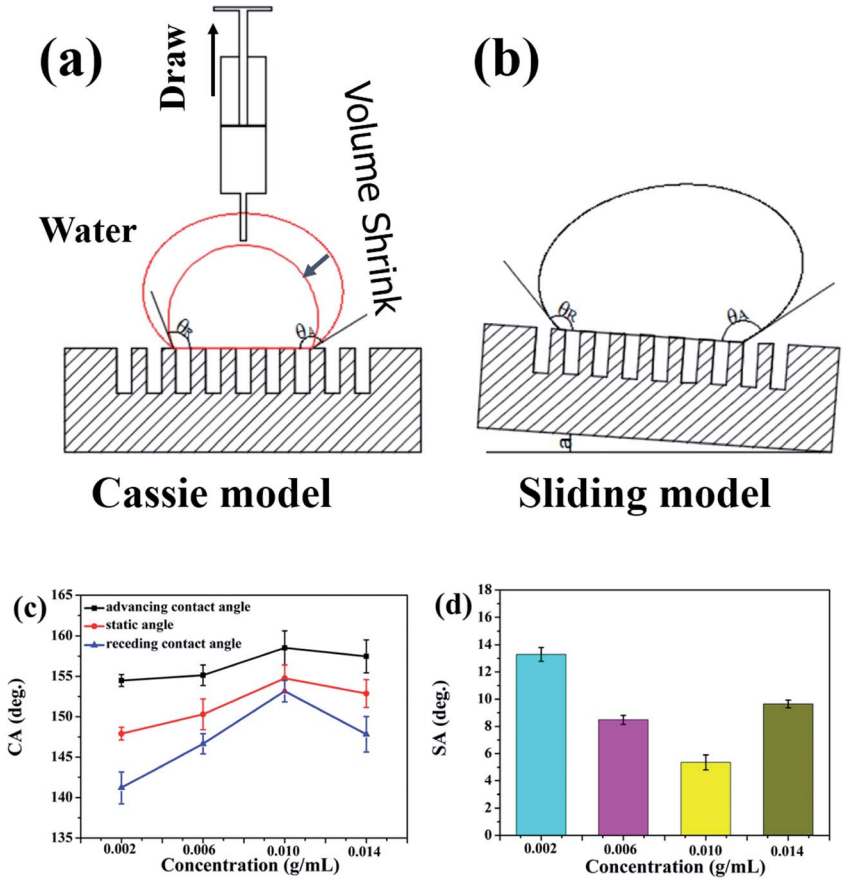

Fig. 5 (a) Schematic diagram of the advancing and receding contact angles θ_A and θ_R, respectively, for a droplet deposited on the rough metal mesh surface. (b) Schematic diagram of the sliding angle of the droplet. (c) Variations in the apparent contact angle, advancing contact angle and receding contact angle for different solution concentrations. (d) Mesh sliding angle for different solution concentrations.

the concentration of the PDMS solution, the droplet shape became oblate owing to gravity. Therefore, the apparent contact angle and sliding angle increased first and then decreased with an increase in the concentration of the PDMS solution, as shown in Fig. 5(c) and (d).

To study the dynamic wetting behavior of water and oil during permeation on the mesh, a video contact angle measurement system was used to record the adhesion and fast permeation of a liquid droplet (5 μL). Fig. 6(a) shows images of a water droplet (5 μL) contacting and leaving the sample. A water droplet was forced to contact the mesh and to detach from the surface after a significant deformation. Therefore, the obtained mesh was confirmed to exhibit excellent superhydrophobicity and low water adhesion. In the case of the permeation of oil, as shown in Fig. 6(b), when an oil droplet (5 μL) contacted the mesh it completed the wetting process quickly and the CA approached zero in ~2.3 s. However, a water droplet (5 μL) easily rolled off the mesh surface in a very short time, as shown in Fig. 6(c), which demonstrated that the superhydrophobic coated mesh had a very low sliding angle.

The electrodeposition of copper and chemical modification with PDMS were considered to improve the durability of the superhydrophobicity. Mesh/Cu/PDMS-coated, if used on the sea, will suffer from the effects of the marine environment.

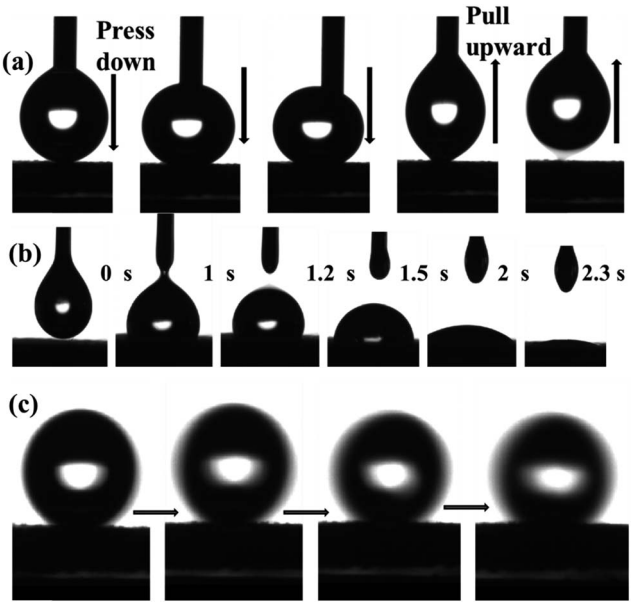

Fig. 6 (a) Dynamic contact and departure process for a water droplet (5 μL). The arrows show the direction of movement of the water droplet. (b) Photographs of dynamic measurements of the wettability by oil of the obtained mesh. (c) Sliding process for water droplet (5 μL) on the obtained mesh.

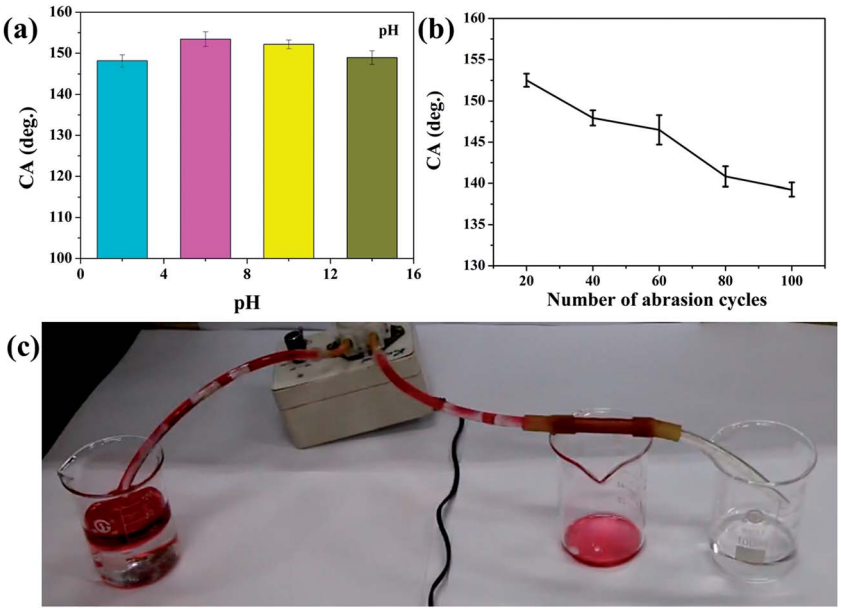

Fig. 7 (a) Mechanical durability of mesh/Cu/PDMS-coated. The CA of mesh/Cu/PDMS-coated was measured after immersion in solutions with different pH values for 3 days. (b) CAs of mesh/Cu/PDMS-coated during abrasion cycling tests. (c) Photograph of the continuous collection of pure oil from an oil/water mixture with the experimental apparatus.

Corrosion reactions with dissolution of the metal can occur in both basic and acidic solutions. The stable durability and robustness of the superhydrophobic mesh were evaluated *via* exposure to different conditions. The obtained mesh was immersed in aqueous solutions with different pH values (2, 6, 10, and 14) for 3 days while measuring the CA and SA (Fig. S6†) before and after changing the pH values. As shown in Fig. S2† and 7(a), the CA remained unchanged, which indicated strong resistance to acid or alkali because of air trapped on mesh/Cu/PDMS-coated.

Antiabrasion properties play an important role in testing superhydrophobic materials for practical applications. The mechanical durability of mesh/Cu/PDMS-coated was evaluated *via* abrasion cycling tests. As shown in Fig. 7(b), abrasion tests on mesh/Cu/PDMS-coated were conducted with a load of 1 kg on 400 grid SiC sandpaper. SEM images after six cycles of abrasion are shown in Fig. S3.† Further analysis showed that the CA of a water droplet on mesh/Cu/PDMS-coated decreased from 155.63° to 139.24° after 100 cycles of abrasion, as shown in Fig. 7(b). However, it is not obvious that there was a decreasing trend in hydrophobic properties over multiple abrasion cycles. To some extent, robust nanostructures were damaged, which caused a decrease in the CA of a water droplet. The result showed that mesh/Cu/PDMS-coated could retain excellent hydrophobicity after multiple abrasion cycles.

To further study the separation ability of mesh/Cu/PDMS-coated based on the obtained mesh, as shown in Fig. 7(c), pure oil can leak into a beaker and water can pass through from the mesh because of its superhydrophobicity and superoleophilicity, which shows that a vacuum pump can achieve the recycling of oil automatically and continuously.

4. Conclusions

In conclusion, we have fabricated a robust and porous mesh with superhydrophobic and superoleophilic characteristics *via* a simple method comprising the electrodeposition of Cu thin films and chemical modification with PDMS. Mesh/Cu/PDMS-coated films displayed CAs of ~155.63° for a water droplet and ~0° for an oil droplet. Then, we conducted experiments by immersion in solutions of different pH values and abrasion tests. The mesh retained stable, excellent superhydrophobic properties. Using the mesh, a vacuum pump could achieve the recycling of oil automatically and continuously, which could be effectively used for the separation of oil/water mixtures.

Acknowledgements

The authors would like to acknowledge the Primary Research & Development Plan of Shanxi Province (Grant No. 201603D121002-2) for the financial support.

References

1 Z. Xu, K. Miyazaki and T. Hori, Fabrication of polydopamine-coated superhydrophobic fabrics for oil/water separation and self-cleaning, *Appl. Surf. Sci.*, 2016, **370**, 243–251.
2 Q. Shang and Y. Zhou, Fabrication of transparent superhydrophobic porous silica coating for self-cleaning and anti-fogging, *Ceram. Int.*, 2016, **42**, 8706–8712.
3 S. P. Fu, R. P. Sahu, E. Diaz, J. R. Robles, C. Chen and X. Rui, Dynamic Study of Liquid Drop Impact on Supercooled Cerium Dioxide: Anti-Icing Behavior, *Langmuir*, 2016, **32**, 6148–6162.

4 S. Farhadi, M. Farzaneh and S. A. Kulinich, Anti-icing performance of superhydrophobic surfaces, *Appl. Surf. Sci.*, 2011, **257**, 6264–6269.
5 N. Miljkovic and E. N. Wang, Condensation heat transfer on superhydrophobic surfaces, *MRS Bull.*, 2013, **38**, 397–406.
6 M. Sheikholeslami, M. Gorji-Bandpy and D. D. Ganji, Review of heat transfer enhancement methods: Focus on passive methods using swirl flow devices, *Renewable Sustainable Energy Rev.*, 2015, **49**, 444–469.
7 H. Zhang, L. Yin, X. Liu, R. Weng, Y. Wang and Z. Wu, Wetting behavior and drag reduction of superhydrophobic layered double hydroxides films on aluminum, *Appl. Surf. Sci.*, 2016, **380**, 178–184.
8 B. R. Solomon, K. S. Khalil and K. K. Varanasi, Drag reduction using lubricant-impregnated surfaces in viscous laminar flow, *Langmuir*, 2014, **30**, 10970–10976.
9 H. K. Raut, S. S. Dinachali, Y. C. Loke, R. Ganesan, K. K. Ansah-Antwi, A. Góra, E. H. Khoo, V. A. Ganesh, M. S. M. Saifullah and S. Ramakrishna, Multiscale Ommatidial Arrays with Broadband and Omnidirectional Antireflection and Antifogging Properties by Sacrificial Layer Mediated Nanoimprinting, *ACS Nano*, 2015, **9**, 9.
10 C.-W. Peng, K.-C. Chang, C.-J. Weng, M.-C. Lai, C.-H. Hsu and S.-C. Hsu, Nano-casting technique to prepare polyaniline surface with biomimetic superhydrophobic structures for anticorrosion application, *Electrochim. Acta*, 2013, **95**, 192–199.
11 V. Fateev, O. Alekseeva, E. Lutikova, V. Porembskiy, S. Nikitin and A. Mikhalev, New physical technologies for catalyst synthesis and anticorrosion protection, *Int. J. Hydrogen Energy*, 2016, **41**, 10515–10521.
12 E. Bormashenko and V. Starov, Impact of surface forces on wetting of hierarchical surfaces and contact angle hysteresis, *Colloid Polym. Sci.*, 2012, **291**, 343–346.
13 E. Bormashenko, R. Grynyov, G. Chaniel, H. Taitelbaum and Y. Bormashenko, Robust technique allowing manufacturing superoleophobic surfaces, *Appl. Surf. Sci.*, 2013, **270**, 98–103.
14 C.-H. Xue, P.-T. Ji, P. Zhang, Y.-R. Li and S.-T. Jia, Fabrication of superhydrophobic and superoleophilic textiles for oil–water separation, *Appl. Surf. Sci.*, 2013, **284**, 464–471.
15 J. Zhu, B. Liu, L. Li, Z. Zeng, W. Zhao and G. Wang, Simple and Green Fabrication of a Superhydrophobic Surface by One-Step Immersion for Continuous Oil/Water Separation, *J. Phys. Chem. A*, 2016, **120**, 5617–5623.
16 H. Peng, H. Wang, J. Wu, G. Meng, Y. Wang and Y. Shi, Preparation of Superhydrophobic Magnetic Cellulose Sponge for Removing Oil from Water, *Ind. Eng. Chem. Res.*, 2016, **55**, 832–838.
17 W. Zhang, Z. Shi, F. Zhang, X. Liu, J. Jin and L. Jiang, Superhydrophobic and superoleophilic PVDF membranes for effective separation of water-in-oil emulsions with high flux, *Adv. Mater.*, 2013, **25**, 2071–2076.
18 X. Gao, L. P Xu, Z. Xue, L. Feng, J. Peng and Y. Wen, Dual-scaled porous nitrocellulose membranes with underwater superoleophobicity for highly efficient oil/water separation, *Adv. Mater.*, 2014, **26**, 1771–1775.
19 B. Li, L. Wu, L. Li, S. Seeger, J. Zhang and A. Wang, Superwetting double-layer polyester materials for effective removal of both insoluble oils and soluble dyes in water, *ACS Appl. Mater. Interfaces*, 2014, **6**, 11581–11588.
20 Y. Wan, B. Wang, J. S. Khim, S. Hong, W. J. Shim and J. Hu, Naphthenic acids in coastal sediments after the Hebei Spirit oil spill: a potential indicator for oil contamination, *Environ. Sci. Technol.*, 2014, **48**, 4153–4162.
21 Z. Xue, Y. Cao, N. Liu, L. Feng and L. Jiang, Special wettable materials for oil/water separation, *J. Mater. Chem. A*, 2014, **2**, 2445–2460.
22 W. Zhang, Y. Zhu, X. Liu, D. Wang, J. Li and L. Jiang, Salt-induced fabrication of superhydrophilic and underwater superoleophobic PAA-*g*-PVDF membranes for effective separation of oil-in-water emulsions, *Angew. Chem., Int. Ed. Engl.*, 2014, **53**, 856–860.
23 R. Gao, Q. Liu, J. Wang, J. Liu, W. Yang and Z. Gao, Construction of superhydrophobic and superoleophilic nickel foam for separation of water and oil mixture, *Appl. Surf. Sci.*, 2014, **289**, 417–424.
24 B. Wang, J. Li, G. Wang, W. Liang, Y. Zhang and L. Shi, Methodology for robust superhydrophobic fabrics and sponges from *in situ* growth of transition metal/metal oxide nanocrystals with thiol modification and their applications in oil/water separation, *ACS Appl. Mater. Interfaces*, 2013, **5**, 1827–1839.
25 Q. Zhu, Y. Chu, Z. Wang, N. Chen, L. Lin and F. Liu, Robust superhydrophobic polyurethane sponge as a highly reusable oil-absorption material, *J. Mater. Chem. A*, 2013, **1**, 5386.
26 X. Lin, F. Lu, Y. Chen, N. Liu, Y. Cao and L. Xu, One-step breaking and separating emulsion by tungsten oxide coated mesh, *ACS Appl. Mater. Interfaces*, 2015, **7**, 8108–8113.
27 J. Li, R. Kang, Y. Zhang, M. Li, H. She and F. Zha, Facile fabrication of superhydrophobic meshes with different water adhesion and their influence on oil/water separation, *RSC Adv.*, 2016, **6**, 90824–90830.
28 B. Song, Simple and fast fabrication of superhydrophobic metal wire mesh for efficiently gravity-driven oil/water separation, *Mar. Pollut. Bull.*, 2016, **113**, 211–215.
29 D. Tian, X. Zhang, J. Zhai and L. Jiang, Photocontrollable water permeation on the micro/nanoscale hierarchical structured ZnO mesh films, *Langmuir*, 2011, **27**, 4265–4270.
30 A. K. Kota, Y. Li, J. M. Mabry and A. Tuteja, Hierarchically structured superoleophobic surfaces with ultralow contact angle hysteresis, *Adv. Mater.*, 2012, **24**, 5838–5843.
31 S. L. Pesek, Y.-H. Lin, H. Z. Mah, W. Kasper, B. Chen and B. J. Rohde, Synthesis of bottlebrush copolymers based on poly(dimethylsiloxane) for surface active additives, *Polymer*, 2016, **98**, 495–504.
32 M. A. Gondal, M. S. Sadullah, M. A. Dastageer, G. H. McKinley, D. Panchanathan and K. K. Varanasi, Study of factors governing oil–water separation process using TiO(2) films prepared by spray deposition of

nanoparticle dispersions, *ACS Appl. Mater. Interfaces*, 2014, **6**, 13422–13429.

33 H. Zhang, W. Li, D. Cui, Z. Hu and L. Xu, Design of lotus-simulating surfaces: Thermodynamic analysis based on a new methodology, *Colloids Surf., A*, 2012, **413**, 314–327.

34 S. A. Seyedmehdi, H. Zhang and J. Zhu, Fabrication of superhydrophobic coatings based on nanoparticles and fluoropolyurethane, *J. Appl. Polym. Sci.*, 2013, **128**, 4136–4140.

35 C. L. Xu, L. Fang, F. Wu, Q. L. Huang and B. Yin, Wetting behavior of triethoxyoctylsilane modified ZnO nanowire films, *Colloids Surf., A*, 2014, **444**, 48–53.